The *Mycobacterium marinum* ESX-1 system mediates phagosomal permeabilization and type I interferon production via separable mechanisms

Julia Lienard[a], Esther Nobs[a], Victoria Lovins[a,1], Elin Movert[b], Christine Valfridsson[b], and Fredric Carlsson[a,2]

[a]Department of Biology, Section for Molecular Cell Biology, Lund University, 223 62 Lund, Sweden; and [b]Department of Experimental Medical Science, Section for Immunology, Lund University, 221 84 Lund, Sweden

Edited by William R. Jacobs Jr, Albert Einstein College of Medicine, Bronx, NY, and approved November 27, 2019 (received for review July 8, 2019)

Following mycobacterial entry into macrophages the ESX-1 type VII secretion system promotes phagosomal permeabilization and type I IFN production, key features of tuberculosis pathogenesis. The current model states that the secreted substrate ESAT-6 is required for membrane permeabilization and that a subsequent passive leakage of extracellular bacterial DNA into the host cell cytosol is sensed by the cyclic GMP-AMP synthase (cGAS) and stimulator of IFN genes (STING) pathway to induce type I IFN production. We employed a collection of *Mycobacterium marinum* ESX-1 transposon mutants in a macrophage infection model and show that permeabilization of the phagosomal membrane does not require ESAT-6 secretion. Moreover, loss of membrane integrity is insufficient to induce type I IFN production. Instead, type I IFN production requires intact ESX-1 function and correlates with release of mitochondrial and nuclear host DNA into the cytosol, indicating that ESX-1 affects host membrane integrity and DNA release via genetically separable mechanisms. These results suggest a revised model for major aspects of ESX-1–mediated host interactions and put focus on elucidating the mechanisms by which ESX-1 permeabilizes host membranes and induces the type I IFN response, questions of importance for our basic understanding of mycobacterial pathogenesis and innate immune sensing.

mycobacterial pathogenesis | ESAT-6 secretion | membrane permeabilization | mitochondrion | type I interferon

Mycobacterium tuberculosis has an intracellular lifestyle and is thought to reside primarily in host macrophages (1). During the 1970s the concept emerged that the bacterium propagates exclusively within the phagosomal compartment, made possible by bacterial mechanisms to prevent phagosome maturation and acidification (2, 3). However, recent work has established that pathogenic mycobacteria can rupture the phagosomal membrane in an ESX-1–dependent manner to interact also with the cytosolic compartment of infected cells in vitro (4–8) and in vivo (6, 9).

The conserved ESX-1 secretion system is primarily encoded by genes within and adjacent to the chromosomal locus "region of difference 1" (RD1), which is defined by a corresponding deletion in the *Mycobacterium bovis* bacillus Calmette–Guérin vaccine strain (10–12). Loss of RD1 is largely responsible for the attenuated phenotype of bacillus Calmette–Guérin (13), and genetic studies in both *M. tuberculosis* and *M. marinum* have confirmed a critical role for ESX-1 in intracellular growth and virulence (9, 14–17). ESAT-6 (EsxA) and CFP-10 (EsxB) are encoded within RD1 and represent the two most well-known substrates of ESX-1 (11). There is a substantial body of work—based on both genetic (4, 5, 8, 10, 17) and biochemical (17–20) approaches—suggesting that ESX-1–mediated permeabilization of the phagosomal membrane requires secretion of ESAT-6, which has been ascribed membranolytic activity by functioning as a pore-forming protein (17, 20–22). Moreover, induction of the type I IFN response, which is exploited by mycobacteria to promote infection (23–25), has been described as a direct and inescapable consequence of phagosomal permeabilization. According to this model, ESX-1–mediated permeabilization of the phagosomal membrane causes passive leakage of extracellular mycobacterial DNA into the host cell cytosol, where it is sensed by the cGAS/STING pathway to drive type I IFN production (24, 26–29). Thus, it is widely believed that ESAT-6 is directly responsible for phagosomal permeabilization and a subsequent default induction of type I IFN during mycobacterial infection.

Results

Analyses of ESAT-6 and CFP-10 Secretion Identify 3 Phenotypic Groups among ESX-1–Deficient Mutants. To determine the genetic requirements for ESX-1–mediated secretion of ESAT-6 and CFP-10 we employed wild-type (WT) *M. marinum* and the ΔRD1 strain, lacking the entire RD1 region, as well as 9 previously characterized isogenic transposon mutants deficient for individual ESX-1–related genes (Fig. 1*A*). Cultures of these strains were fractionated into the secreted fraction (culture filtrate; CF), cell envelope fraction (ENV), and cytosolic fraction (CYT), which were analyzed by Western blot (Fig. 1*B*). As controls we probed for Ag85B, which is secreted via the general secretory pathway, and the cell-associated protein GroEL. Although these controls did not distinguish between the envelope and cytosolic fractions, they demonstrated similar loading and lack of unspecific leakage of cellular material into the CF, respectively (Fig. 1*B*).

Significance

The mycobacterial ESX-1 type VII secretion system promotes phagosomal rupture and type I IFN production, key features of tuberculosis pathogenesis. It is currently believed that the secreted substrate ESAT-6 is required for phagosomal permeabilization and that a subsequent leakage of bacterial DNA into the host cell cytosol triggers type I IFN. Our genetic analyses demonstrate that ESX-1–mediated membrane permeabilization does not require ability to secrete ESAT-6 and is insufficient to induce type I IFN. Instead, type I IFN production is associated with intact ESX-1 function and correlates with cytosolic release of host DNA. Thus, ESX-1 affects host membrane integrity and induction of type I IFN via discrete mechanisms. Understanding these mechanisms may provide insight into how mycobacteria cause disease.

Author contributions: J.L. and F.C. designed research; J.L., E.N., V.L., E.M., C.V., and F.C. performed research; J.L., E.N., V.L., E.M., C.V., and F.C. analyzed data; and J.L. and F.C. wrote the paper.

The authors declare no competing interest.

This article is a PNAS Direct Submission.

[1]Present address: Department of Dermatology, Perelman School of Medicine, University of Pennsylvania, Philadelphia, PA 19104.

[2]To whom correspondence may be addressed. Email: fredric.carlsson@biol.lu.se.

This article contains supporting information online at https://www.pnas.org/lookup/suppl/doi:10.1073/pnas.1911646117/-/DCSupplemental.

First published December 26, 2019.

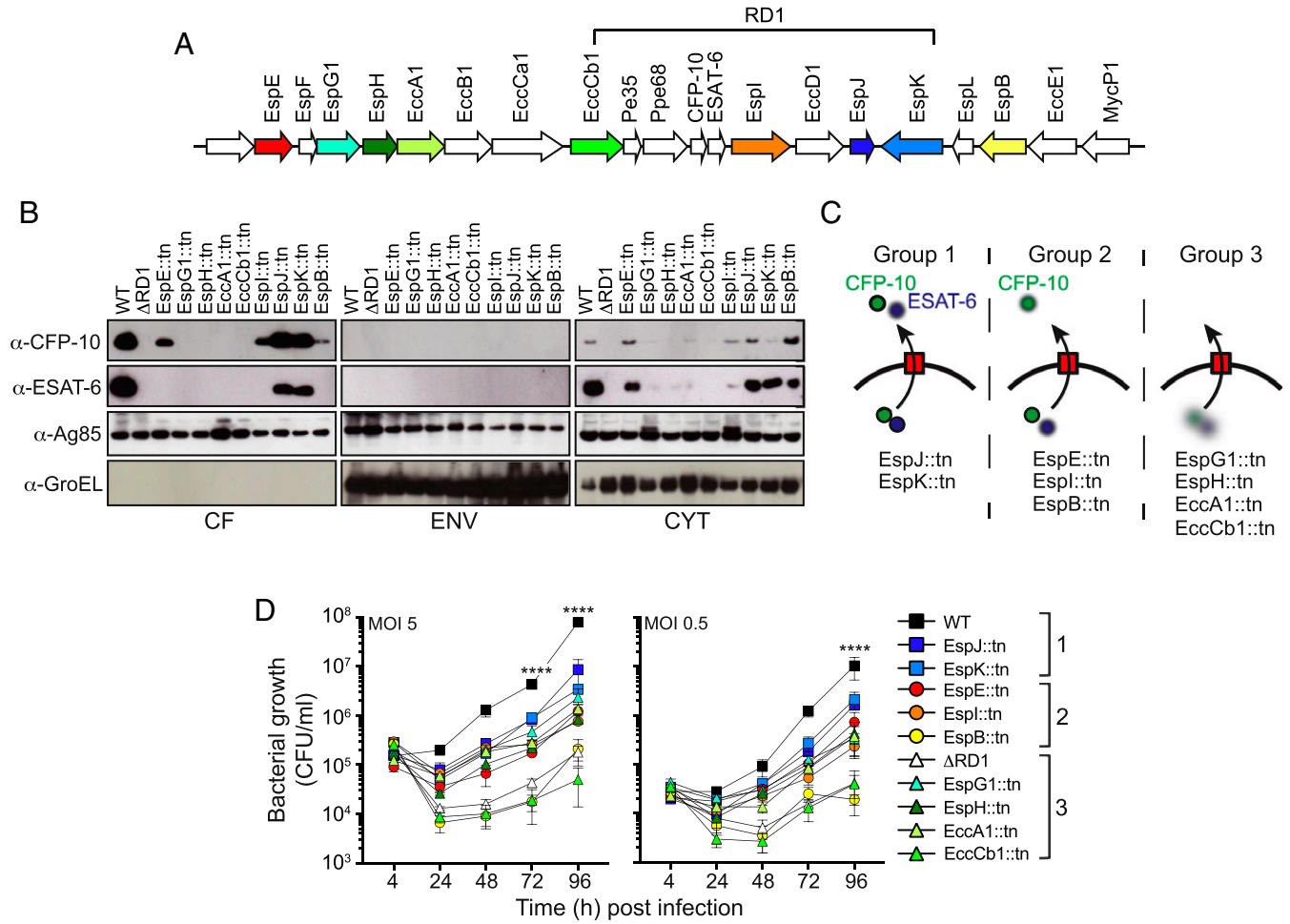

Fig. 1. Analyses of ESAT-6 and CFP-10 secretion delineate 3 phenotypic groups of ESX-1 mutants. (*A*) Schematic representation of the extended RD1 region of mycobacteria. Arrows represent individual genes with direction of transcription, and the colors highlight the transposon mutants used in this study (*SI Appendix*, Table S1). (*B*) *M. marinum* bacterial cultures of WT, ΔRD1, and the indicated transposon insertion mutants were fractionated into secreted (culture filtrates; CF), cell envelope (ENV), and cytosolic (CYT) fractions and analyzed by Western blot using specific antibodies. Ag85, a protein secreted by the general secretory pathway, and GroEL, a cell-associated protein, were used as controls. (*C*) Schematic representation of the 3 phenotypic groups of *M. marinum* strains identified based on their ability to secrete ESAT-6 and CFP-10. (*D*) C57BL/6 macrophages were infected with *M. marinum* at the indicated MOI, and intracellular bacterial growth was determined by cfu analyses at the indicate time points post infection. Phenotypic groups 1, 2, and 3 are indicated. Results (mean ± SD; $n = 3$) are representative of 3 independent experiments (2-way ANOVA, $^{****}P < 0.0001$).

As expected, WT but not ΔRD1 produced and secreted ESAT-6 and CFP-10 (Fig. 1*B*). Intriguingly, among the transposon mutants we identified three principal phenotypic groups based on their ability to secrete ESAT-6 and CFP-10, respectively (Fig. 1 *B* and *C*). First, EspJ::tn and EspK::tn secreted both ESAT-6 and CFP-10, albeit at reduced levels as compared to WT (Fig. 1*B*). Of note, these findings partly contrast with a previous study, in which the EspJ::tn and EspK::tn mutants were not observed to secrete ESAT-6 (10), a discrepancy that might be explained by differences in how the bacterial fractions were generated. Second, EspE::tn, EspI::tn, and, to a lesser degree, EspB::tn secreted CFP-10 while being unable to secrete ESAT-6 (Fig. 1*B*), implying utility of these mutants as reagents to investigate the mechanism by which ESAT-6 piggybacks on CFP-10 for its secretion (30). Third, EspG1::tn, EspH::tn, EccA1::tn, and EccCb1::tn failed to secrete both ESAT-6 and CFP-10, a phenotype associated with markedly reduced cytosolic levels of the substrates (Fig. 1*B*). Importantly, these findings provided a unique opportunity to experimentally investigate the role for ESAT-6 secretion in ESX-1–mediated functions during physiological infection of macrophages.

Analysis of intracellular growth in C57BL/6 bone marrow-derived macrophages demonstrated that EccCb1::tn and EspB::tn exhibited a severe growth defect similar to that of ΔRD1 (Fig. 1*D*). All other mutants exhibited an intermediate phenotype irrespective of their capacity to secrete ESAT-6 (Fig. 1*D*). The growth phenotype for ESX-1 mutants in our system appeared stronger than that observed in the *M. tuberculosis* system (15, 31), which might reflect the faster growth rate of *M. marinum* or potentially differences in the ESX-1 systems from the two species (32). Nevertheless, the lack of correlation between ESX-1–mediated intracellular growth and ESAT-6 secretion in addition to a lack of belonging to any phenotypic group made it of interest to further explore the role for ESAT-6 secretion in ESX-1–mediated functions.

ESX-1–Mediated Permeabilization of the Phagosomal Membrane Does Not Require ESAT-6 Secretion. After permeabilizing the phagosomal membrane and gaining access to the host cell cytosol, *M. marinum* is able to induce actin tail formation at one of its polar ends (7). To investigate the role for ESAT-6 secretion in ESX-1–mediated permeabilization of the phagosomal membrane we employed three strains from each phenotypic group and performed kinetic and quantitative immunofluorescence microscopy analysis to determine the fraction of infected macrophages containing actin tail-associated bacteria (Fig. 2 *A* and *B*). To this end we

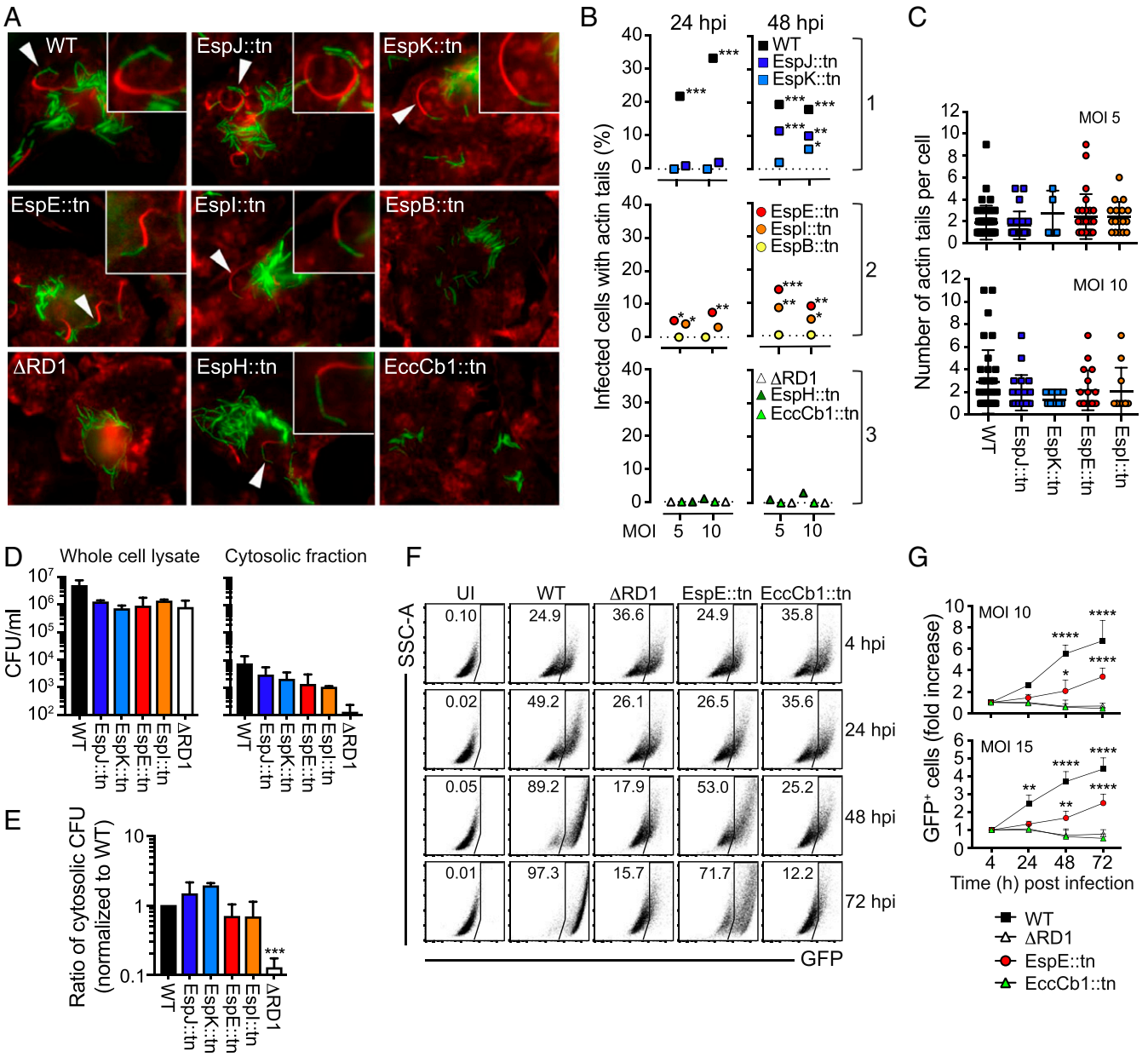

Fig. 2. ESX-1–mediated permeabilization of the phagosomal membrane does not require ESAT-6 secretion. (*A*–*C*) Macrophages were infected with WT *M. marinum* and mutant strains (green) as indicated and stained for polymerized actin (red phalloidin) at 24 and 48 h post infection (hpi). (*A*) Presence of actin tails analyzed by microscopy. Arrows indicate actin tail-associated bacteria. (*B*) Quantification of the fraction of infected cells with actin tails. Data based on 1 experiment, representative of 2 independent experiments, where at least 200 infected cells were analyzed per condition. χ^2 test (*<0.05; **<0.01; ***<0.001), compared to ΔRD1. (*C*) Number of actin tails per cell (at 48 hpi) among actin tail-containing infected cells, as indicated. No significant differences between groups (one-way ANOVA). (*D* and *E*) Macrophages were infected at MOI = 5 as indicated, and the number of cfus in whole cell lysates and cytosolic fractions, respectively, was determined at 48 hpi. (*D*) cfus from whole cell lysates and cytosolic fractions. (*E*) The ratio of cytosolic cfus over total cfus (in whole cell extracts), normalized to WT. Results (mean + SD; $n = 3$) are representative of 3 independent experiments (one-way ANOVA, ***$P < 0.001$). No statistical difference between WT and the transposon mutants. (*F* and *G*) Macrophages were infected with GFP-expressing bacteria as indicated, and intercellular bacterial spread was analyzed by flow cytometry. (*F*) Representative plots of GFP-positive macrophages (infected at MOI = 10) at different hpi. Uninfected cells (UI) were analyzed as a control. Side scatter (SSC-A) and GFP, as indicated. (*G*) Graph shows the fold increase of GFP$^+$ cells compared to 4 hpi. Results (mean + SD) from 3 independent experiments (2-way ANOVA, **$P < 0.01$, ****$P < 0.0001$).

had available WT, ΔRD1, EspE::tn, and EccCb1::tn that carry a chromosomal insertion of *gfp* in the *attB* site (33, 34), enabling visualization, and EspJ::tn, EspK::tn, EspI::tn, EspB::tn, and EspH::tn were transformed with a plasmid encoding the green fluorescent protein "Wasabi." Consistent with the critical role for ESX-1 in phagosomal rupture, WT but not ΔRD1 induced actin tails at both 24 and 48 h post infection (hpi; Fig. 2 *A* and *B*). EspJ::tn and EspK::tn were able to generate actin tails, although with a delayed kinetics and to a lesser degree compared to WT (Fig. 2 *A* and *B*). Surprisingly, EspE::tn and EspI::tn exhibited more robust actin tail formation than EspJ::tn and EspK::tn (Fig. 2 *A* and *B*), indicating that ESX-1–mediated rupture of the phagosomal membrane does not require ESAT-6 secretion. Moreover, comparative analysis of individual actin tail-containing cells infected with WT, EspJ::tn, EspK::tn, EspE::tn, and EspI::tn showed that these

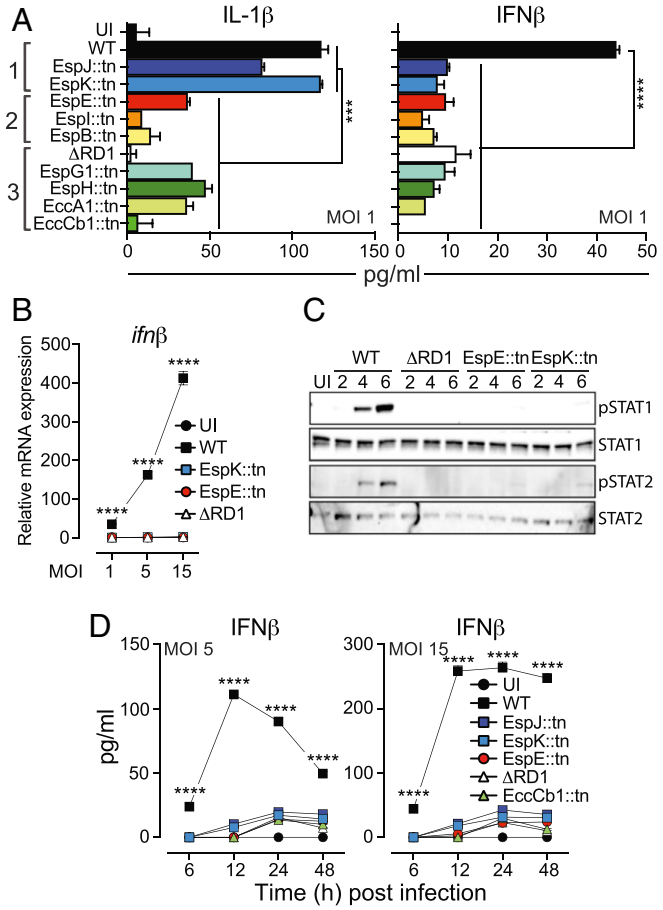

Fig. 3. Phagosomal permeabilization is not sufficient to induce type I IFN production. Macrophages were infected with WT *M. marinum* and mutant strains as indicated. Uninfected (UI) cells were analyzed as control. (*A*) Culture supernatants were collected at 24 hpi and analyzed for the indicated cytokines. Phenotypic groups 1, 2, and 3 are indicated. Results (mean + SD; $n = 3$) are representative of at least 3 independent experiments. Statistical significance (one-way ANOVA, $***P < 0.001$, $****P < 0.0001$) as indicated. In addition, infection with EspJ::tn caused reduced ($P < 0.001$) IL-1β secretion as compared to WT and EspK::tn. (*B*) Macrophages were harvested at 4 hpi, and *ifnβ* mRNA was measured by RT-qPCR. Data are represented as a fold-change relative to the UI control. Results (mean ± SD; $n = 3$) are representative of 3 independent experiments (2-way ANOVA, $****P < 0.0001$). (*C*) Infected macrophages (MOI = 5) were lysed at 2, 4 and 6 hpi and analyzed for STAT1 and STAT2 activation by Western blot. Detection of activated (i.e., phosphorylated) transcription factors was performed using phosphospecific primary antibodies (pSTAT1 and pSTAT2). Shown is 1 experiment representative of 2. (*D*) Kinetic analysis of IFNβ secretion from macrophages infected as indicated. Results (mean ± SD; $n = 3$) are representative of 3 independent experiments (2-way ANOVA, $****P < 0.0001$).

mutants and WT generated similar numbers of actin tails per macrophage (Fig. 2*C*).

Although Western blots are not truly quantitative, our analyses suggested that the bacterial cytosol of EspB::tn contained more ESAT-6 protein than that of EspI::tn and similar amounts as that of EspE::tn (Fig. 1*B*). The finding that EspB::tn was unable to rupture the phagosomal membrane, as indicated by lack of actin tails (Fig. 2 *A* and *B*), suggests that leakage of ESAT-6 from the bacterial cytosol does not explain the ability of EspE::tn and EspI::tn to permeabilize the phagosome. It is also noteworthy that EspH::tn, which essentially did not contain any ESAT-6 or CFP-10 (Fig. 1*B*), was observed to induce actin tails, albeit at a very low level (Fig. 2 *A* and *B*).

To separately assess the requirement for ESAT-6 secretion in gaining access to the cytosol we performed parallel colony-forming unit (cfu) analyses of whole cell extracts and enriched cytosolic fractions from infected macrophages (Fig. 2*D*) and calculated the ratio of cytosolic over total cfus (Fig. 2*E*). ΔRD1 had an ∼10-fold lower ratio of cytosolic cfus compared to WT bacteria (Fig. 2*E*), providing the analytical window for ESX-1 in this assay. Remarkably, the ratios for EspJ::tn and EspK::tn as well as for EspE::tn and EspI::tn were similar to that of WT (Fig. 2*E*), indicating that ESX-1–mediated phagosome rupture occurs via an ESAT-6 secretion-independent mechanism.

To further explore whether ESAT-6 secretion is dispensable for rupture of the phagosomal membrane we analyzed intercellular bacterial spread (Fig. 2 *F* and *G*), a process linked to the membranolytic activity of ESX-1 (10). For this purpose we performed kinetic experiments of macrophages infected with WT, ΔRD1, EspE::tn, and EccCb1::tn—i.e., the strains encoding *gfp* chromosomally and exhibiting comparable fluorescence (*SI Appendix*, Fig. S1)—and identified infected macrophages as green fluorescent protein (GFP)-positive by flow cytometry (Fig. 2*F*). Consistent with our analyses of actin tails and cytosolic cfus (Fig. 2 *A*–*E*), EspE::tn was able to spread among macrophages, although at a lower level compared to WT bacteria (Fig. 2 *F* and *G*). As expected, both ΔRD1 and EccCb1::tn were unable to spread (Fig. 2 *F* and *G*). Collectively, our results (Fig. 2 *A*–*G*) support the interpretation that ESAT-6 secretion is not required for ESX-1–mediated phagosomal permeabilization in infected macrophages.

Permeabilization of the Phagosomal Membrane Is Not Sufficient to Drive the Type I IFN Response. Analyses of the immune regulatory functions of ESX-1 suggested that IL-1β secretion largely correlated with proficient secretion of ESAT-6 and CFP-10 (Fig. 3 *A*, *Left*), whereas none of the mutants were able to drive secretion of IFNβ (Fig. 3 *A*, *Right*), supporting the idea that ESX-1 drives inflammasome activation and the type I IFN response via genetically separable mechanisms (27). Importantly, because EspJ::tn and EspK::tn as well as EspE::tn and EspI::tn were able to rupture the phagosome (Fig. 2) these results indicate that neither ESAT-6 secretion nor permeabilization of the phagosomal membrane is sufficient to induce the cGAS/STING-signaling pathway. To validate this finding we focused on EspK::tn and EspE::tn from phenotypic groups 1 and 2, respectively. Gene expression analysis of macrophages infected at different multiplicities of infection (MOI) demonstrated that *M. marinum* drives transcription of *ifnβ* in an ESX-1– and dose-dependent manner (Fig. 3*B*). Similarly to ΔRD1, however, both EspK::tn and EspE::tn failed to induce *ifnβ* expression (Fig. 3*B*). Consistently, macrophages infected with EspK::tn and EspE::tn did not provoke ESX-1–mediated type I IFN receptor-signaling, as determined by analyses of STAT1 and STAT2 phosphorylation (Fig. 3*C*). Finally, kinetic analyses confirmed that EspK::tn and EspE::tn were completely unable to drive ESX-1–mediated IFNβ secretion (Fig. 3*D*). Thus, ESX-1–mediated phagosomal membrane permeabilization is insufficient to drive the type I IFN response.

ESX-1 promotes cytotoxicity to infected cells (17), which might impact on cytokine output, prompting us to investigate the ability of EspK::tn and EspE::tn to kill infected macrophages. Kinetic flow cytometry-based analysis of Zombie-staining demonstrated that EspK::tn and EspE::tn induced cell death similarly to WT bacilli (*SI Appendix*, Fig. S2 *A* and *B*). Analysis of LDH release confirmed that both EspK::tn and EspE::tn compromised cellular integrity, albeit at a lower level than WT (*SI Appendix*, Fig. S2*C*). The unique ability of WT *M. marinum* to induce the type I IFN response is therefore likely not a consequence of differential cell death. Of note, phagosomal rupture by mycobacteria has been linked to host cell death (4, 5), which is implicated in bacterial spread (35, 36). Consistent with this notion our analyses implied similar genetic requirements for cytotoxicity (*SI Appendix*, Fig. S2) and spread (Fig. 2 *F* and *G*).

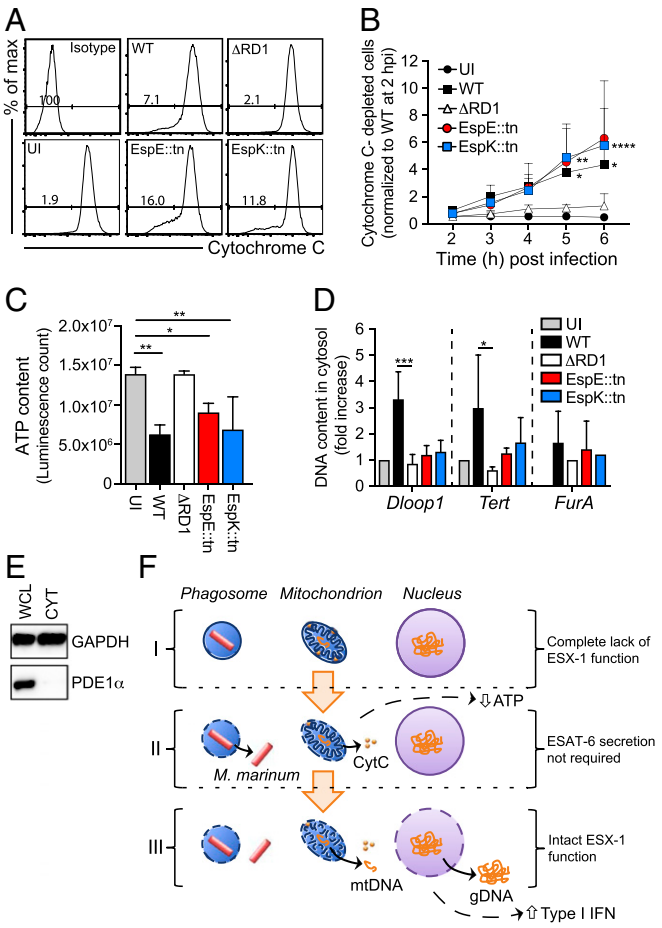

Fig. 4. ESX-1–dependent disruption of mitochondrial integrity and cytosolic DNA release are genetically separate mechanisms. (*A* and *B*) Macrophages were infected as indicated at MOI = 15, and kinetic experiments of Cytochrome C (CytC) release were performed by flow cytometry. An isotype IgG antibody and UI cells were analyzed as controls. (*A*) The histogram plots show the cell counts (*y* axis) and the fluorescence intensity (*x* axis) as well as the percentage of cells negative for CytC-staining, i.e., cells with CytC depletion, at 6 hpi. (*B*) The graph represents the fold increase of CytC-depleted cells. Data normalized to WT *M. marinum* at 2 hpi. Results (mean + SD) from 4 independent experiments (2-way ANOVA, $*P < 0.05$, $**P < 0.01$, $****P < 0.0001$). (*C*) Macrophages were infected as indicated at MOI = 15, and total ATP was measured at 24 hpi using a luminescent assay. Results (mean + SD) from 3 independent experiments (one-way ANOVA, $*P < 0.05$, $**P < 0.01$). (*D*) Macrophages were infected as indicated at MOI = 5. UI cells were analyzed as control. The presence of mitochondrial (*Dloop1*), nuclear (*Tert*), or mycobacterial (*FurA*) DNA in the cytosolic compartment was evaluated by qPCR at 24 hpi. Results (mean + SD) from 3 independent experiments (one-way ANOVA, $*P < 0.05$, $***P < 0.001$). (*E*) The mitochondrial protein puryvate dehydrogenase E1 alpha (PDE1α) was analyzed in whole cell lysates (WCL) and cytosolic fractions (CYT) by Western blot. GAPDH was used as a loading control. Shown is 1 experiment representative of 2. (*F*) Schematic representation illustrating that *M. marinum* infection of macrophages can be separated into at least 3 distinct stages (I–III) based on an incremental need for ESX-1 functionality. Genomic (gDNA) and mitochondrial (mtDNA) DNA, as indicated.

ESX-1 Affects Mitochondrial Integrity and DNA Release into the Host Cell Cytosol via Genetically Separable Mechanisms. Previous reports have suggested that ESX-1 interferes with mitochondrial integrity (37–39) and that release of mitochondrial DNA into the host cell cytosol may serve as the trigger for the cGAS/STING pathway in *M. tuberculosis*-infected macrophages (40). We therefore sought to probe the functional interaction between ESX-1 and mitochondria during infection.

Cytochrome C (CytC) resides in the intermembrane region of intact mitochondria and leaks out into the cytosol upon rupture of the outer membrane. Using a flow cytometry-based assay (*SI Appendix*, Fig. S3) we investigated CytC depletion in macrophages infected with WT, ΔRD1, EspK::tn, or EspE::tn as a measure of their ability to disrupt the integrity of the outer mitochondrial membrane. Analyses of WT and ΔRD1 demonstrated that *M. marinum* ruptures the outer membrane in an ESX-1–dependent fashion (Fig. 4 *A* and *B*). Permeabilization of the outer membrane did not distinguish WT from EspK::tn or EspE::tn as they caused a similar depletion of CytC (Fig. 4 *A* and *B*), further demonstrating that ESX-1–mediated membrane permeabilization does not require ESAT-6 secretion. These mutants and WT similarly reduced the ATP content of infected macrophages (Fig. 4*C*), an expected consequence of decoupling the respiratory chain by outer membrane permeabilization (Fig. 4 *A* and *B*), and of cytotoxicity (*SI Appendix*, Fig. S2). Thus, the genetic requirements for rupturing the outer mitochondrial (Fig. 4 *A* and *B*) and phagosomal (Fig. 2) membranes are similar, and loss of integrity of these membranes is insufficient to induce type I IFN production (Fig. 3).

To investigate the genetic requirements for ESX-1–mediated release of DNA into the cytosol we purified the cytosolic compartment of infected macrophages and performed qPCR-based analyses of mitochondrial (*Dloop1*), nuclear (*Tert*), and bacterial (*FurA*) DNA (Fig. 4*D*). The purity of our cytosolic fractions was confirmed by Western blot analysis of the mitochondrial protein PDE1α (Fig. 4*E*). In agreement with previous reports (40, 41), *M. marinum* mobilized detectable levels of mitochondrial and nuclear, but not bacterial, DNA into the macrophage cytosol in an ESX-1–dependent manner (Fig. 4*D*). Importantly, however, this ability was lost in both EspK::tn and EspE::tn (Fig. 4*D*), possibly explaining why only WT induces type I IFN production (Fig. 3). ESX-1–mediated release of host DNA into the cytosolic compartment was independent of type I IFN receptor-signaling (*SI Appendix*, Fig. S4), consistent with DNA mobilization acting upstream of the type I IFN response. These findings establish the mitochondrion as a key target for ESX-1 via at least two genetically separable mechanisms and identify mobilization of host DNA into the cytosol as a correlate to the ability of the WT ESX-1 system to induce type I IFN production.

Discussion

ESAT-6 and CFP-10 are cotranscribed, and the proteins physically interact in the bacterial cytosol, where CFP-10 is responsible for targeting the heterodimer to the ESX-1 apparatus for secretion (11, 30). The membranolytic property of ESAT-6 was first proposed based on the findings that an *M. tuberculosis* transposon insertion mutant in the CFP-10 encoding gene was unable to lyse macrophages as well as lung epithelial cells and that purified ESAT-6, but not CFP-10, was able to disrupt lipid bilayers (17). While it is possible that the mode of secretion might be different for bacteria in infected cells as compared to those in the growth medium used by us and others, genetic analyses in *M. tuberculosis* (4, 5, 8) and *M. marinum* (10) have established a strong correlation between ESAT-6 secretion and host membrane permeabilization. Studies with purified protein have further suggested that ESAT-6 alone is sufficient to lyse membranes by functioning as a pore-forming protein (17, 20–22). Importantly, the biochemical basis for the model outlined above was recently questioned by the findings that the lytic activity of purified ESAT-6 may be due to residual detergent in the protein preparation and that ESAT-6 is not sufficient to permeabilize the phagosomal membrane in *M. marinum*-infected macrophages (42). Moreover, conclusions drawn from the genetic studies are confounded by the observation that several ESX-1 proteins are codependent for their stability and secretion (33, 43–45), making classical genetic approaches to establish requirement for specific

gene products inherently difficult. Our genetic approach enabled us to demonstrate that the ability to secrete ESAT-6 is not required for permeabilization of the phagosomal and outer mitochondrial membranes, suggesting the existence of an ESAT-6 secretion-independent mechanism underlying ESX-1–mediated host membrane permeabilization (Fig. 4*F*). We speculate that this may include unrecognized membranolytic effector functions, or a functional interplay between ESX-1 and other bacterial structures. For example, EccA1 has been shown to regulate the rate of mycolic acid synthesis in *M. marinum* (46), and phthiocerol dimycocerosates of the *M. tuberculosis* cell wall may reduce membrane fluidity (47) and potentiate the membranolytic effect of ESX-1 (48), suggesting functional relationships between ESX-1 and mycobacterial cell wall lipids, some of which may affect phagosomal rupture. Moreover, *Rickettsia* disrupts the phagosomal membrane via production of phospholipase A2 (49), and *M. tuberculosis* has been proposed to regulate the activation of cytosolic host phospholipase A2 (50), leaving open the possibility that ESX-1 might regulate host factors such as lipolytic enzymes. Interestingly, our results also suggest that mycobacterial infection of macrophages can be delineated into at least three distinct stages, which can be placed in a hierarchical order based on an incremental need for ESX-1 functionality (Fig. 4*F*)—opening an avenue to investigate ESX-1–mediated virulence mechanisms at a level of detail previously not possible in physiological infection.

Pathogenic mycobacteria exploit the type I IFN axis to promote infection (23–25, 51). *M. tuberculosis* and *M. marinum* induce type I IFN production via the cGAS and STING pathway in an ESX-1–dependent manner (24, 26–29, 41). Double-stranded DNA of any origin can act as a cofactor to activate the cytosolically located cGAS to synthesize 2′, 3′-cGMP-AMP, a cyclic dinucleotide acting as a second messenger to activate STING, which in turn drives type I IFN production via TANK-binding kinase 1 (TBK1)- and IFN regulatory factor 3 (IRF3)-signaling (52). It is generally believed that ESX-1–mediated permeabilization of bacteria-containing phagosomes leads to the release of extracellular mycobacterial DNA into the host cell cytosol where it is sensed by cGAS to induce the type I IFN response (24, 26–29). Nevertheless, it was recently proposed that *M. tuberculosis* and *M. marinum* mobilize mitochondrial and nuclear, but not bacterial, DNA into the host cell cytosol in an ESX-1–dependent manner (40, 41) and that mitochondria-derived DNA is causally responsible for cGAS activation (40). We find that loss of membrane integrity is insufficient to induce type I IFN production in infected macrophages (Fig. 4*F*), suggesting that a possible passive leakage of bacterial DNA is not sufficient to trigger cGAS activation. Instead, type I IFN production correlates with a measurable release of mitochondrial and nuclear host DNA (Fig. 4*F*). The inability of EspK::tn, EspJ::tn, EspE::tn, and EspI::tn—which are able to permeabilize host membranes—to induce type I IFN production suggests that a genetically separable, and as of yet unidentified, ESX-1–mediated function is required to release host DNA into the cytosol (Fig. 4*F*). Thus, ESX-1 affects membrane integrity and DNA release via discrete mechanisms, and the molecular events underlying the required role for ESX-1 in cGAS activation and type I IFN production remain to be understood. It will be of interest to explore these findings in the context of *M. tuberculosis* as well as human macrophages. In light of our results it may also be of interest to revisit the mechanism of cGAS activation during infection with other pathogens on the growing list of bacteria that induce type I IFN production via the cGAS/STING pathway (52), where it is often believed that bacteria-derived DNA acts as the trigger.

We hope that our work will stimulate research aimed at elucidating the molecular details of how ESX-1 permeabilizes host membranes and induces the type I IFN response, open questions of great importance for our basic understanding of mycobacterial pathogenesis and innate immune sensing.

Materials and Methods

All of the materials and experimental procedures used are described in detail in *SI Appendix*. Reagents, including bacterial strains, are listed in *SI Appendix*, Table S1. Animal care and use adhered to the Swedish animal welfare laws and to the guidelines set by the Swedish Department of Agriculture (Act 1988:534). These studies were approved by the Malmö/Lund Ethical Board for Animal Research (permit numbers M9-13 and M45-15).

ACKNOWLEDGMENTS. We acknowledge the Biodefence and Emerging Infections Research Resources Repository (BEI Resources) for reagents and Jonatan Regander for technical assistance. These studies were supported by grants from the Swedish Research Council (Dnr: 2018-04777, to F.C.), the Knut and Alice Wallenberg Foundation (to F.C.), as well as the foundations of Emil and Wera Cornell (to F.C.), Alfred Österlunds (to F.C.), Sigurd and Elsa Golje (to J.L., E.M., and F.C.), and the Royal Physiographic Society in Lund (to J.L., E.M., and F.C.).

1. C. J. Cambier, S. Falkow, L. Ramakrishnan, Host evasion and exploitation schemes of *Mycobacterium tuberculosis*. *Cell* **159**, 1497–1509 (2014).
2. J. A. Armstrong, P. D. Hart, Response of cultured macrophages to *Mycobacterium tuberculosis*, with observations on fusion of lysosomes with phagosomes. *J. Exp. Med.* **134**, 713–740 (1971).
3. M. B. Goren, P. D'Arcy Hart, M. R. Young, J. A. Armstrong, Prevention of phagosome-lysosome fusion in cultured macrophages by sulfatides of *Mycobacterium tuberculosis*. *Proc. Natl. Acad. Sci. U.S.A.* **73**, 2510–2514 (1976).
4. D. Houben *et al.*, ESX-1-mediated translocation to the cytosol controls virulence of mycobacteria. *Cell Microbiol.* **14**, 1287–1298 (2012).
5. R. Simeone *et al.*, Phagosomal rupture by *Mycobacterium tuberculosis* results in toxicity and host cell death. *PLoS Pathog.* **8**, e1002507 (2012).
6. R. Simeone *et al.*, Cytosolic access of *Mycobacterium tuberculosis*: Critical impact of phagosomal acidification control and demonstration of occurrence in vivo. *PLoS Pathog.* **11**, e1004650 (2015).
7. L. M. Stamm *et al.*, *Mycobacterium marinum* escapes from phagosomes and is propelled by actin-based motility. *J. Exp. Med.* **198**, 1361–1368 (2003).
8. N. van der Wel *et al.*, *M. tuberculosis* and *M. leprae* translocate from the phagolysosome to the cytosol in myeloid cells. *Cell* **129**, 1287–1298 (2007).
9. F. Carlsson *et al.*, Host-detrimental role of Esx-1-mediated inflammasome activation in mycobacterial infection. *PLoS Pathog.* **6**, e1000895 (2010).
10. L. Y. Gao *et al.*, A mycobacterial virulence gene cluster extending RD1 is required for cytolysis, bacterial spreading and ESAT-6 secretion. *Mol. Microbiol.* **53**, 1677–1693 (2004).
11. M. I. Gröschel, F. Sayes, R. Simeone, L. Majlessi, R. Brosch, ESX secretion systems: Mycobacterial evolution to counter host immunity. *Nat. Rev. Microbiol.* **14**, 677–691 (2016).
12. T. P. Stinear *et al.*, Insights from the complete genome sequence of Mycobacterium marinum on the evolution of *Mycobacterium tuberculosis*. *Genome Res.* **18**, 729–741 (2008).
13. A. S. Pym, P. Brodin, R. Brosch, M. Huerre, S. T. Cole, Loss of RD1 contributed to the attenuation of the live tuberculosis vaccines *Mycobacterium bovis* BCG and *Mycobacterium microti*. *Mol. Microbiol.* **46**, 709–717 (2002).
14. K. M. Guinn *et al.*, Individual RD1-region genes are required for export of ESAT-6/CFP-10 and for virulence of *Mycobacterium tuberculosis*. *Mol. Microbiol.* **51**, 359–370 (2004).
15. S. A. Stanley, S. Raghavan, W. W. Hwang, J. S. Cox, Acute infection and macrophage subversion by *Mycobacterium tuberculosis* require a specialized secretion system. *Proc. Natl. Acad. Sci. U.S.A.* **100**, 13001–13006 (2003).
16. H. E. Volkman *et al.*, Tuberculous granuloma formation is enhanced by a mycobacterium virulence determinant. *PLoS Biol.* **2**, e367 (2004).
17. T. Hsu *et al.*, The primary mechanism of attenuation of bacillus Calmette-Guerin is a loss of secreted lytic function required for invasion of lung interstitial tissue. *Proc. Natl. Acad. Sci. U.S.A.* **100**, 12420–12425 (2003).
18. M. I. de Jonge *et al.*, ESAT-6 from *Mycobacterium tuberculosis* dissociates from its putative chaperone CFP-10 under acidic conditions and exhibits membrane-lysing activity. *J. Bacteriol.* **189**, 6028–6034 (2007).
19. S. C. Derrick, S. L. Morris, The ESAT6 protein of *Mycobacterium tuberculosis* induces apoptosis of macrophages by activating caspase expression. *Cell Microbiol.* **9**, 1547–1555 (2007).
20. J. Smith *et al.*, Evidence for pore formation in host cell membranes by ESX-1-secreted ESAT-6 and its role in *Mycobacterium marinum* escape from the vacuole. *Infect. Immun.* **76**, 5478–5487 (2008).
21. X. Peng *et al.*, Characterization of differential pore-forming activities of ESAT-6 proteins from *Mycobacterium tuberculosis* and *Mycobacterium smegmatis*. *FEBS Lett.* **590**, 509–519 (2016).
22. A. Refai *et al.*, Two distinct conformational states of *Mycobacterium tuberculosis* virulent factor early secreted antigenic target 6 kDa are behind the discrepancy around its biological functions. *FEBS J.* **282**, 4114–4129 (2015).
23. C. Manca *et al.*, Virulence of a *Mycobacterium tuberculosis* clinical isolate in mice is determined by failure to induce Th1 type immunity and is associated with induction of IFN-alpha /beta. *Proc. Natl. Acad. Sci. U.S.A.* **98**, 5752–5757 (2001).
24. P. S. Manzanillo, M. U. Shiloh, D. A. Portnoy, J. S. Cox, *Mycobacterium tuberculosis* activates the DNA-dependent cytosolic surveillance pathway within macrophages. *Cell Host Microbe* **11**, 469–480 (2012).

25. S. A. Stanley, J. E. Johndrow, P. Manzanillo, J. S. Cox, The Type I IFN response to infection with *Mycobacterium tuberculosis* requires ESX-1-mediated secretion and contributes to pathogenesis. *J. Immunol.* **178**, 3143–3152 (2007).
26. A. C. Collins *et al*., Cyclic GMP-AMP synthase is an innate immune DNA sensor for *Mycobacterium tuberculosis*. *Cell Host Microbe* **17**, 820–828 (2015).
27. R. Wassermann *et al*., *Mycobacterium tuberculosis* differentially activates cGAS- and inflammasome-dependent intracellular immune responses through ESX-1. *Cell Host Microbe* **17**, 799–810 (2015).
28. R. O. Watson, P. S. Manzanillo, J. S. Cox, Extracellular *M. tuberculosis* DNA targets bacteria for autophagy by activating the host DNA-sensing pathway. *Cell* **150**, 803–815 (2012).
29. R. O. Watson *et al*., The cytosolic sensor cGAS detects *Mycobacterium tuberculosis* DNA to induce type I interferons and activate autophagy. *Cell Host Microbe* **17**, 811–819 (2015).
30. P. A. Champion, S. A. Stanley, M. M. Champion, E. J. Brown, J. S. Cox, C-terminal signal sequence promotes virulence factor secretion in *Mycobacterium tuberculosis*. *Science* **313**, 1632–1636 (2006).
31. D. Bottai *et al*., ESAT-6 secretion-independent impact of ESX-1 genes espF and espG1 on virulence of *Mycobacterium tuberculosis*. *J. Infect. Dis.* **203**, 1155–1164 (2011).
32. M. I. Gröschel *et al*., Recombinant BCG expressing ESX-1 of *Mycobacterium marinum* combines low virulence with cytosolic immune signaling and improved TB protection. *Cell Rep.* **18**, 2752–2765 (2017).
33. F. Carlsson, S. A. Joshi, L. Rangell, E. J. Brown, Polar localization of virulence-related Esx-1 secretion in mycobacteria. *PLoS Pathog.* **5**, e1000285 (2009).
34. B. McLaughlin *et al*., A mycobacterium ESX-1-secreted virulence factor with unique requirements for export. *PLoS Pathog.* **3**, e105 (2007).
35. S. M. Behar, M. Divangahi, H. G. Remold, Evasion of innate immunity by *Mycobacterium tuberculosis*: Is death an exit strategy? *Nat. Rev. Microbiol.* **8**, 668–674 (2010).
36. A. H. Moraco, H. Kornfeld, Cell death and autophagy in tuberculosis. *Semin. Immunol.* **26**, 497–511 (2014).
37. M. Chen, H. Gan, H. G. Remold, A mechanism of virulence: Virulent *Mycobacterium tuberculosis* strain H37Rv, but not attenuated H37Ra, causes significant mitochondrial inner membrane disruption in macrophages leading to necrosis. *J. Immunol.* **176**, 3707–3716 (2006).
38. L. Duan, H. Gan, D. E. Golan, H. G. Remold, Critical role of mitochondrial damage in determining outcome of macrophage infection with *Mycobacterium tuberculosis*. *J. Immunol.* **169**, 5181–5187 (2002).
39. K. Fine-Coulson, S. Giguère, F. D. Quinn, B. J. Reaves, Infection of A549 human type II epithelial cells with *Mycobacterium tuberculosis* induces changes in mitochondrial morphology, distribution and mass that are dependent on the early secreted antigen, ESAT-6. *Microbes Infect.* **17**, 689–697 (2015).
40. K. E. Wiens, J. D. Ernst, The mechanism for type I interferon induction by *Mycobacterium tuberculosis* is bacterial strain-dependent. *PLoS Pathog.* **12**, e1005809 (2016).
41. E. Movert *et al*., Streptococcal M protein promotes IL-10 production by cGAS-independent activation of the STING signaling pathway. *PLoS Pathog.* **14**, e1006969 (2018).
42. W. H. Conrad *et al*., Mycobacterial ESX-1 secretion system mediates host cell lysis through bacterium contact-dependent gross membrane disruptions. *Proc. Natl. Acad. Sci. U.S.A.* **114**, 1371–1376 (2017).
43. M. M. Champion, E. A. Williams, R. S. Pinapati, P. A. Champion, Correlation of phenotypic profiles using targeted proteomics identifies mycobacterial esx-1 substrates. *J. Proteome Res.* **13**, 5151–5164 (2014).
44. S. M. Fortune *et al*., Mutually dependent secretion of proteins required for mycobacterial virulence. *Proc. Natl. Acad. Sci. U.S.A.* **102**, 10676–10681 (2005).
45. C. Sala *et al*., EspL is essential for virulence and stabilizes EspE, EspF and EspH levels in *Mycobacterium tuberculosis*. *PLoS Pathog.* **14**, e1007491 (2018).
46. S. A. Joshi *et al*., EccA1, a component of the *Mycobacterium marinum* ESX-1 protein virulence factor secretion pathway, regulates mycolic acid lipid synthesis. *Chem. Biol.* **19**, 372–380 (2012).
47. C. Astarie-Dequeker *et al*., Phthiocerol dimycocerosates of *M. tuberculosis* participate in macrophage invasion by inducing changes in the organization of plasma membrane lipids. *PLoS Pathog.* **5**, e1000289 (2009).
48. J. Augenstreich *et al*., ESX-1 and phthiocerol dimycocerosates of *Mycobacterium tuberculosis* act in concert to cause phagosomal rupture and host cell apoptosis. *Cell Microbiol.* **19**, e12726 (2017).
49. D. H. Walker, H. M. Feng, V. L. Popov, Rickettsial phospholipase A2 as a pathogenic mechanism in a model of cell injury by typhus and spotted fever group rickettsiae. *Am. J. Trop. Med. Hyg.* **65**, 936–942 (2001).
50. S. V. Jamwal *et al*., Mycobacterial escape from macrophage phagosomes to the cytoplasm represents an alternate adaptation mechanism. *Sci. Rep.* **6**, 23089 (2016).
51. A. Dorhoi *et al*., Type I IFN signaling triggers immunopathology in tuberculosis-susceptible mice by modulating lung phagocyte dynamics. *Eur. J. Immunol.* **44**, 2380–2393 (2014).
52. Q. Chen, L. Sun, Z. J. Chen, Regulation and function of the cGAS-STING pathway of cytosolic DNA sensing. *Nat. Immunol.* **17**, 1142–1149 (2016).